*Desalination and Water Treatment*
www.deswater.com
doi: 10.5004/dwt.2023.29338

286 (2023) 217–227
February

# Modeling of pesticide adsorption on fixed-bed column using biomaterials: response surface methodology optimization

Abdelhamid Bakka[a,*], Hamza Saffaj[b], Khalid Aziz[a], Hamid Zidouh[a], Taoufiq Saffaj[c], Faissal Aziz[d], Imane Adraoui[a], Rachid Mamouni[a,*], Nabil Saffaj[a,*]

[a]*Laboratory of Biotechnology, Materials and Environment (LBME), Department of Chemistry, Faculty of Sciences, Ibn Zohr University – BP 8106, Agadir, Morocco, emails: abdelhamid.bakka@gmail.com (A. Bakka), azizkhalid710@gmail.com (K. Aziz), Hamid.zidouh@gmail.com (H. Zidouh), adraouiimane2020@gmail.com (I. Adraoui), r.mamouni@uiz.ac.ma (R. Mamouni), saffaj@gmail.com (N. Saffaj)*
[b]*Laboratory of Algebra Analysis and Applications, Department of Mathematics and Computer, Faculty of Sciences Ben M'Sik, University Hassan II, Casablanca, Morocco, email: saffajhamza@gmail.com*
[c]*Laboratory of Applied Organic Chemistry, University Sidi Mohamed Ben Abdellah, Fes, Morocco, email: saffajt@gmail.com*
[d]*Laboratory of Water, Biodiversity and Climate Changes, Faculty of Science Semlalia, Cadi Ayyad University, B.P. 2390, 40000, Marrakech, Morocco, email: f.aziz@uca.ma*

Received 4 November 2022; Accepted 29 January 2023

**ABSTRACT**

Dynamic adsorption of bifenthrin pesticide onto treated gari tellinella shells (TGTS) was investigated using fixed-bed column technique. Response surface methodology based on Box–Behnken design has been used to study the influence operation parameters on the adsorption. Our main goal is to optimize the process at lower cost with maximum efficiency, identification of influential factors to the process, the evaluation of interactions between these factors and modeling mathematical result. The properties of TGTS biosorbent are determined by the application of X-ray diffraction, Fourier-transform infrared spectroscopy, scanning electron microscopy/energy-dispersive X-ray spectroscopy, thermogravimetric analysis/differential thermal analysis, $pH_{pzc}$ and Brunauer–Emmett–Teller characterization techniques. TGTS is composed of a calcium carbonate ($CaCO_3$) phase and has a specific surface area equal to 151 $m^2 \cdot g^{-1}$. In the experiment field study, the amount of bifenthrin adsorbed by TGTS depending on flow rate ($Q$), bed height ($L$), particles size (Ps) and inlet concentration ($C_0$). The coefficients of flow rate, bed height and feed concentration are positive, thus these parameters positively affect the adsorption of bifenthrin onto TGTS biosorbent. Conversely, the particles size coefficient is negative, which means that its influence on the adsorption process is negative. Analysis of variance showed a high coefficient of determination ($R^2$ = 0.958) and satisfactory prediction of the regression model was derived. The largest amount adsorbed (20.73 $mg \cdot g^{-1}$), estimated by a multivariate experimental design, was found under the following optimal experimental conditions: flow rate of 5 mL/min, bed height of 4 cm, particles size of 50 µm, and initial bifenthrin concentration of 12.5 mg/L.

*Keywords:* Bifenthrin; Pesticides; Adsorption; Fixed-bed column; Modelling; Treated gari tellinella shells; Box–Behnken design

* Corresponding author.

## 1. Introduction

Pesticides have been used for decades as an efficient way to control pests in urban and agricultural environments; Nevertheless, their presence in surface water has raised concerns about their potential adverse effects on the ecosystem [1]. The use of pyrethroids for residential and commercial applications has increased significantly in recent years, compared to other commercial pesticides [2]. Pyrethroids are increasingly used in various fields because of their lower toxicity compared to older insecticides such as organochlorines, organophosphates and carbamates, and given their higher efficiency [3]. Despite the toxicity of pyrethroids to humans was considered to be low due to rapid degradation, many studies have proved that metabolites of pyrethroids can have carcinogenic and disruptive effects which can lead to the contamination of various environmental compartments [4].

Various treatment methods, including biodegradation [5], advanced oxidation processes [6], coagulation/flocculation [7], visible-light photocatalytic degradation [8] and adsorption [9] have been used for the removal of pyrethroids from surface and groundwater. Among these different technologies, adsorption has great potential because it has many advantages such as renewable, high performance and simplicity [10]. However, the use of this technology has been found to be limited since it may involve a high investment linked to the cost of the adsorbent material. For example, activated carbon can remove a variety of pollutants, but it is expensive to produce [11]. This is why scientists have taken the initiative to find low-cost, efficient and ecological adsorbents. These works have set up several adsorbents of natural origin called "biosorbent" as-, animal bone [12], chestnut shells [10], egg shells [13] and patellidae shells [14].

Until now, sorption removal of organic compounds such as pharmaceuticals and pesticides from wastewater under specified experimental conditions has been performed in different batch operations. However, batch treatment has several limitations, such as reducing the amount of effluent treated, separation of treated wastewater from adsorbents which made this adsorption system inadequate for scale. These limitations have led some researchers to move towards the adsorption of these compounds on fixed-bed columns under dynamic operating conditions [15–20]. The fixed-bed adsorption process provides an in-depth understanding of mass transfer and the dynamics of breakthrough curves. Modeling the breakthrough process facilitates its optimization under different operating conditions for larger scale applications [19,21].

Conventional and classical methods of investigating the adsorption process on the fixed-bed by varying one factor and keeping the other factors involved at constant unspecified levels do not describe the combined effect of all the factors involved [22]. This method is also time-consuming and requires a large number of experiments to determine optimal levels, which are not reliable. The limitations of conventional methods can be eliminated by collectively optimizing all parameters involved by a statistical design of experiments such as the response surface methodology (RSM) based on the Box–Behnken design. RSM consists of a set of empirical techniques devoted to evaluating the relationships between a group of controlled experimental factors and responses measured according to one or more selected criteria [23,24].

The main objectives of the present paper are: (i) the preparation of low-cost, environment-friendly and efficient biosorbent from treated gari tellinella shells (TGTS), (ii) the characterization of TGTS biosorbent using different analytical methods, and (iii) the prediction of dynamic adsorption behavior of the aldrin pesticide by the Box–Behnken method in order to determine the optimal adsorption design on an industrial scale.

## 2. Materials and methods

### 2.1. Synthesis of TGTS biosorbent

After collecting the gari tellinella shells from the coastal area of Massa City, the shells were washed with distilled water, treated for 10 min with 0.1 M HCl acid, rinsed and placed in the oven at 110°C for 12 h. The shells were crushed using a RETSCH SM10 Laboratory Mill. The obtained powder is treated with NaOH 5% for 5 h at room temperature, rinsed with distilled water to neutralize the pH to 7 and dried at 110°C for 24 h. The produced powder is sieved through a laboratory sieve (Shaker AS 200) to obtain different particles size.

It should be noted that the TGTS, like other biosorbents already used in the literature, can be recycled until they are exhausted and finally TGTS loaded with pollutants can be eliminated by incineration.

### 2.2. Reagents and chemicals

The chemicals used in this study were purchased from Sigma-Aldrich Company Casablanca (Morocco). Bifenthrin has a molecular formula of $C_{23}H_{22}ClF_3O_2$, a molecular weight of 422.87 g/mol and solubility in water of 0.1 mg/L. A stock solution of bifenthrin with a purity of 99.9% was prepared in methanol and kept refrigerated at 3°C until use.

### 2.3. Instrumentation

Maintaining different flow rates in the column was ensured using a Lead Fluid BT300L peristaltic pump. The TGTS biosorbent was characterized by X-ray diffraction (XRD) (PANalytical diffractometer and PANalytical X'Pert HighScore Plus software), analysis by Fourier-transform infrared spectroscopy (FTIR) (JASCO FT/IR-4000), scanning electron microscopy (SEM) (Supra 40 VP COLUMN GEMINI ZEISS coupled with Oxford Instruments X-Max Analyzer) equipped with an energy-dispersive X-ray spectroscopy (EDS) detector, differential thermal and thermogravimetric analysis (Thermogram SHIMADZU DTG60), pH-meter (ISE HI3222 HANNA), and by the Brunauer–Emmett–Teller (BET) method (Nova 2200 Quantachrome Instruments, USA). Samples containing pesticide residues were determined using the Agilent 7890A Gas Chromatograph (GC) equipped with Electron Capture Detector (ECD).

### 2.4. Column experiments

Continuous flow experiments for the removal of bifenthrin pesticide were carried out in fixed-bed columns (glass columns) with an internal diameter of 1 cm and a length of 30 cm. Porous layers of glass wool and glass beads (1.5 mm diameter) were fixed at the top and bottom of the column to ensure a uniform inflow of solution. We investigated the effects of 4 factors according to 3 Box Behnken levels (low, middle and high). To achieve different bed heights of 1, 2.5 and 4 cm, amounts of 0.4, 1 and 1.6 g of TGTS biosorbent was added to the column, respectively. The effects of flow rate (2, 5 and 8 mL/min), bed height (1, 2.5 and 4 cm), particles size (50, 525 and 1,000 μm) and feed concentration (5, 12.5 and 20 mg/L) were studied at room temperature and pH 6. Samples were taken at the column outlet and the bifenthrin concentration was analyzed by gas chromatography coupled with an electron capture detector (GC/ECD).

The total amount of bifenthrin sorbed into the column ($q_{\text{total}}$) is calculated by subtracting the area below the breakthrough curve ($f(t) = C/C_0$) from the exhaustion time ($t_{\text{total}}$), all multiplied by the feed concentration ($C_0$) and flow rate ($Q$) [Eq. (1)] [25].

$$q_{\text{total}} = \frac{Q}{1000}\int_{t=0}^{t=\text{total}}\left(1-\frac{C}{C_0}\right)dt = \frac{QC_0}{1000}\left(t_{\text{total}} - A\right) \quad (1)$$

where $t_{\text{total}}$ is the total flow time (min), $Q$ is the volumetric flow rate (mL/min), $C_0$ and $C$ are the inlet and the outlet pesticide concentration (mg/L), respectively, and $A$ is the area below the breakthrough curve.

## 2.5. Response surface methodology

Response surface methodology is an experimental technique used for predicting and modeling complicated relations between independent factors and one or more responses. In this study, response surface methodology was applied to optimize the adsorption of bifenthrin by TGTS biomaterial. Experiments were performed using Box–Behnken design.

The Box–Behnken design is having the maximum efficiency for a RSM problem involving four factors (flow rate ($Q$), bed height ($L$), particles size (Ps) and initial concentration ($C_0$)). Thus, the number of runs required is low compared to a central composite design. Regarding the measured responses, we retain the adsorbed amounts ($q_{\text{total}}$ expressed in (mg)) of bifenthrin eliminated by the fixed-bed column after the saturation. The process parameters for the study had three levels as given in Table 1. The levels were fixed based on the preliminary experiment trials.

In the optimization process, the response can be related to chosen variables by linear or quadratic models, a quadratic model is given in Eqs. (2) and (3):

Table 1
Process factors and their levels

| Factors | Levels of Box–Behnken | | |
|---|---|---|---|
| | Low (–1) | Middle (0) | High (+1) |
| Flow rate (mL/min) ($X_1$) | 2 | 5 | 8 |
| Bed height (cm) ($X_2$) | 1 | 2.5 | 4 |
| Particles size (μm) ($X_3$) | 50 | 525 | 1,000 |
| Feed concentration (mg/L) ($X_4$) | 5 | 12.5 | 20 |

$$Y = b_0 + \sum_{i=1}^{k} b_i X_i + \sum_{i=1}^{K} b_{ii} X_i^2 + \sum_{i=1}^{k}\sum_{j=1}^{K} b_{ij} X_i X_j + \varepsilon \quad (2)$$

$$\begin{aligned} Y = {} & b_0 + b_1X_1 + b_2X_2 + b_3X_3 + b_4X_4 + b_{12}X_1X_2 + b_{13}X_1X_3 \\ & + b_{14}X_1X_4 + b_{23}X_2X_3 + b_{24}X_2X_4 + b_{34}X_3X_4 + b_{11}X_1^2 \\ & + b_{22}X_2^2 + b_{33}X_3^2 + b_{44}X_4^2 \end{aligned} \quad (3)$$

where $Y$ is the response, $b_0$ is the constant; $b_i$ is the linear coefficient, $b_{ii}$ represents the quadratic coefficient, $b_{ij}$ is the interaction coefficient, $X_i$ is the coded variable level and $i$ or $j$ is the number of the independent variables.

# 3. Results and discussion

## 3.1. Characterization of TGTS biomaterial

The XRD, SEM, EDS, FTIR, $pH_{pzc}$ and BET contributed to the characterization of TGTS. Fig. 1 shows the XRD powder pattern of the synthesized TGTS. 24 peaks including a major peak located at 2θ = 29.47° were revealed. Adjustment of the experimental data with JCPDS No. 96-900-9668 data shows that the TGTS biosorbent consists of a majority phase of calcium carbonate ($CaCO_3$) with a hexagonal crystal system.

The FTIR spectra shown in Fig. 2 reveal the presence of three bands before biosorption and four bands after biosorption. Both FTIR spectra reveal characteristic absorption bands in the 650–1,850 $cm^{-1}$ region corresponding to four types of C–O bond vibrations. The absorption bands before and after biosorption at 713, 875 and 1,450 $cm^{-1}$ are attributed to Ca–O stretching and bending vibrations, respectively [26]. The band at 798 $cm^{-1}$ corresponds to the C–Cl stretching mode [27], confirming the retention of bifenthrin molecules by the surface of TGTS [28].

The elementary analysis shown in Fig. 3 indicates that oxygen is the most representative element (60.72%) followed by calcium (25.19%) and then carbon (14.09%). The high percentage of these three elements confirms that the TGTS biomaterial consists only of calcium carbonate [29].

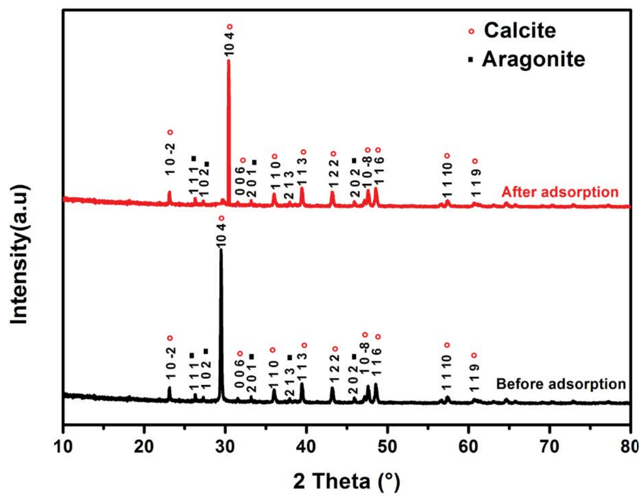


Fig. 1. X-ray diffraction patterns of treated gari tellinella shells biomaterial.

The SEM analysis presented in Fig. 4 shows the ultrastructure of the TGTS biomaterial. Fig. 4a shows the TGTS spectrum before biosorption. It reveals the presence of a porous and heterogeneous surface composed of small particles, which makes it easier for bifenthrin molecules to diffuse and adsorb onto the TGTS surface. Fig. 4b depicts TGTS spectra after biosorption. The presence of large particles and reduced pore size and quality indicates the accumulation of bifenthrin molecules on the TGTS pores [30,31].

The spectra of thermogravimetric analysis/differential thermal analysis (Fig. 5) indicate the presence of four losses. The first (1.9%), which corresponds to the evaporation of bound water, is between 23°C and 190°C. The second (2.0%), corresponding to the removal of organic matter, is between 190°C and 364°C. The third, between 364°C and 483°C (1.2%), corresponds to the loss of the remaining organic matter. And the fourth between 483°C and 877°C (39.8%), corresponding to the $CO_2$ escape. These conclusions show that TGTS biosorbent consists largely of calcium carbonate. Identical results were presented by Wei et al. and Ho et al. [32,33].

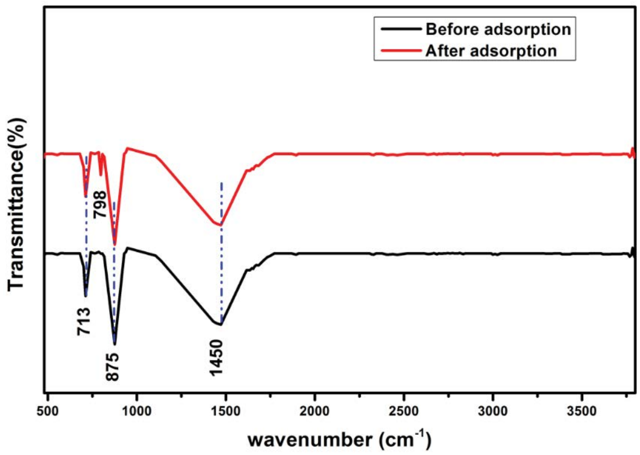


Fig. 2. Fourier-transform infrared spectrum of treated gari tellinella shells biomaterial before and after bifenthrin biosorption.

The $pH_{pzc}$ of TGTS biomaterial was measured according to the methodology proposed by Noh and Schwarz [34]. The results are shown in Fig. 6. It can be seen from the curve that $pH_{pzc}$ is equal to 8.3. Then at pH below 8.3, the TGTS surface is positively charged and can easily adsorb pesticide molecules that are negative. The negative charge of bifenthrin came from the chlorine, fluorine and oxygen atoms. These results confirm the increase in the amount adsorbed under acidic conditions [35].

Fig. 7 shows the results of the adsorption–desorption isotherm measurement of $N_2$. The TGTS isotherm has a behavior characteristic of a type IV isotherm with a hysteresis loop $H_3$ indicating the presence of mesopores. The measured values of the BET surface area, volume, and pore diameter of TGTS were 151 m$^2$/g, 0.09 cm$^3$/g and 35 nm, respectively. The high specific surface area of TGTS results in high removal rates [25].

### 3.2. Experimental design

The proposed Box–Behnken design requires 27 runs for modeling a response surface. Details of the experimental

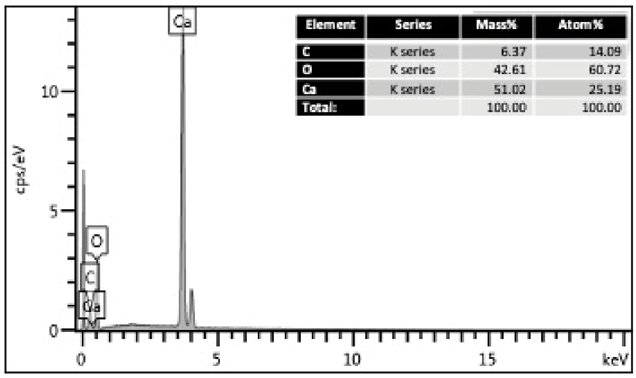


Fig. 3. Energy-dispersive X-ray spectroscopy analysis showing the elementary composition of treated gari tellinella shells biomaterial.

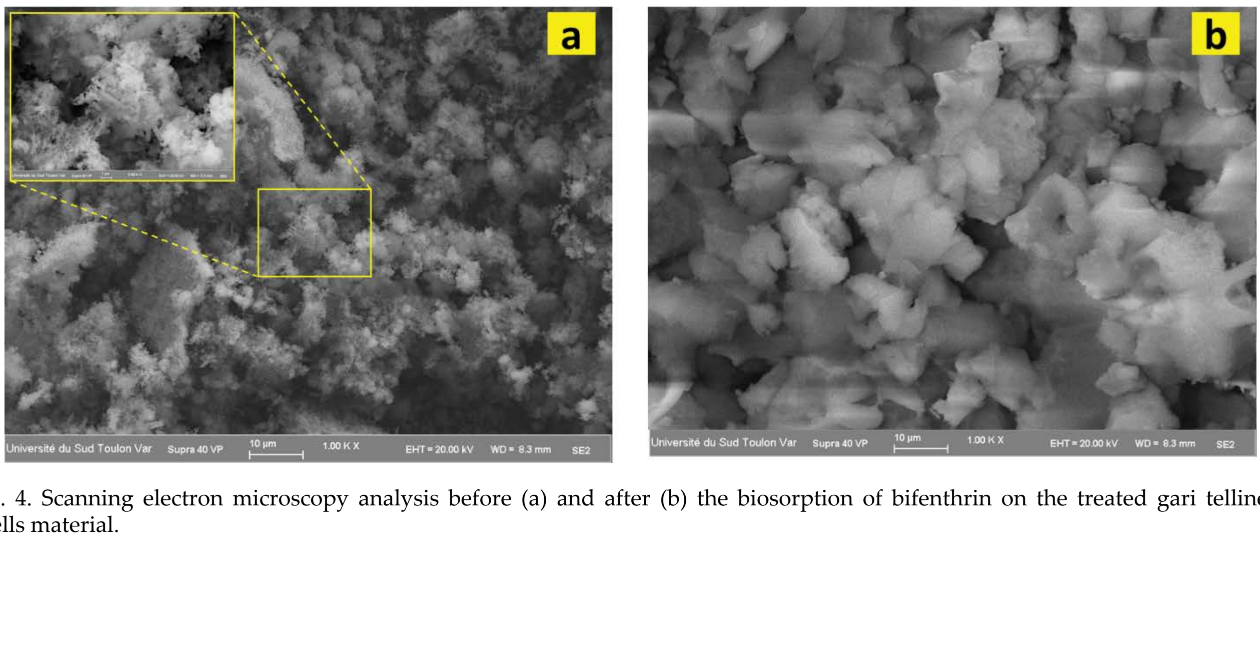


Fig. 4. Scanning electron microscopy analysis before (a) and after (b) the biosorption of bifenthrin on the treated gari tellinella shells material.

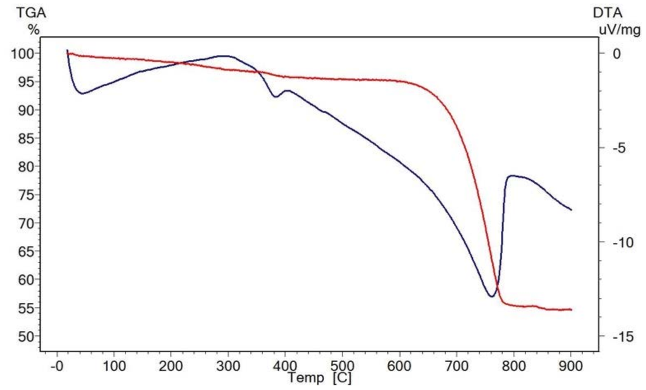


Fig. 5. Thermogravimetric analysis/differential thermal analysis spectrum of treated gari tellinella shells biomaterial.

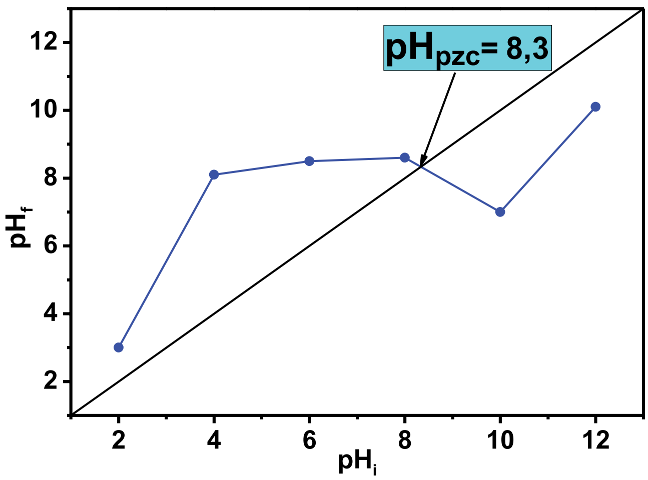


Fig. 6. Experimental determination of $pH_{pzc}$ of treated gari tellinella shells biomaterial.

runs with the set of input parameters that were conducted are given in Table 2. The central point (0, 0, 0, 0) is repeated three times to establish that the experimental data is within the normal dispersion and repeatability is ensured.

Polynomial regression modeling was performed between the response variable $q_{total}$ (mg) and coded values ($X_1$, $X_2$, $X_3$, $X_4$) and the best fitted quadratic polynomial regression model was obtained as follow [Eq. (4)]:

$$Y = 2,967 + 1,561X_1 + 2,402X_2 - 6,501X_3 + 1,513X_4 + X_1X_2 - 2,185X_1X_3 - 3,420X_2X_3 - 2,123X_3X_4 + 4,985X_3^2 \quad (4)$$

Analysis of variance (ANOVA) was employed to investigate the adequacy and significance of the model. The effect of a factor is defined as the change in response produced by a change in the level of the factor. This is frequently called the main effect because it refers to the primary factors of interest in the experiments. The ANOVA results showed that the equation adequately represented the actual relationship between each response and the significant variables. The *F*-value implies that the models are significant and the value of Prob. > *F* less than 0,05 indicates that the model's terms

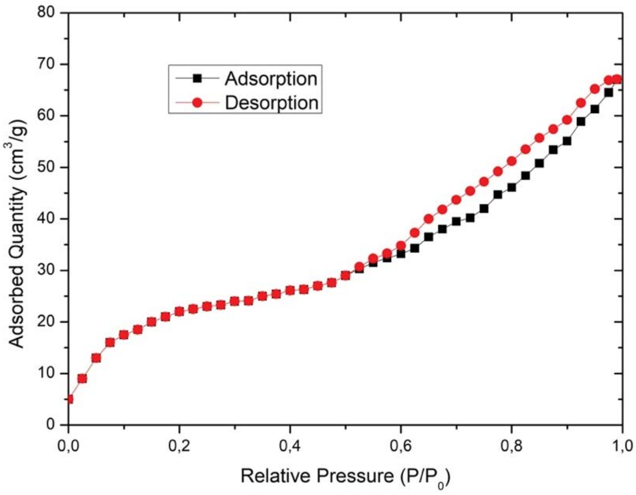


Fig. 7. $N_2$ adsorption–desorption isotherm for treated gari tellinella shells biomaterial.

are significant. Especially larger *F*-value with the associated *p*-value (smaller than 0.05, confidence intervals) means that the experimental system can be modeled effectively with less error.

According to the ANOVA results (Table 4), the value of $F_{cal}$ = 46.85 was higher and the *p*-value was lower than 0.05 which shows the significance and suitability of the quadratic model. Moreover, the normal probability of the residuals almost indicated no departures from the normality (Fig. 8). High coefficient of determination ($R^2$ = 0.958) and adjusted coefficient of determination (Adj. $R^2$ = 0.909) indicate the good agreement of experimental response values with model-predicted values. The predicted *R*-square (0.865) was also in reasonable agreement with adjusted *R*-square and showed a good prediction of the model.

Among all the terms, the linear effects of flow rate (*Q*), bed height (*L*), particles size (Ps) and initial concentration ($C_0$) were found to have a predominant effect on "$q_{total}$" owing to the low *p*-value (<0.05) for the factors. Similarly, the quadratic terms of particles size and the interaction between (flow rate – particles size), (bed height – particles size), (particles size – feed concentration) and dual (feed concentration) were found to be significant owing to their high *F*-values and low *p*-value.

However, the quadratic terms of flow rate, bed height, feed concentration and the interaction between (flow rate – bed height), (bed height – feed concentration) and (flow rate – feed concentration) were not statistically significant on the elimination of bifenthrin by TPS biomaterial.

The graphical interaction between the process parameters was represented using 3-dimensional response surface plots (Figs. 9–11). The interaction between the bed height (*L*) and particles size (Ps) at a constant flow rate (*Q* = 5 mL/min) and feed concentration ($C_0$ = 12.5 mg/L) is shown in Fig. 9. The effect of the interaction between bed height and particles size is significant because by increasing the bed height, the specific surface area involved in the adsorption process also increases. The mass of TGTS adsorbent required increases from 0.4 to 1.6 g to increase the bed height

Table 2
Coefficients estimates and statistics

| Source | Coefficient | F. Inflation | Ecart-type | t. exp. | Signification % |
|---|---|---|---|---|---|
| b0 | 2.967 | – | 1.0395077 | 2.85 | 1.45 |
| b1 | 1.561 | 1.00 | 0.51975383 | 3.00 | 1.10 |
| b2 | 2.402 | 1.00 | 0.51975383 | 4.62 | 0.0589 |
| b3 | –6.501 | 1.00 | 0.51975383 | –12.51 | <0.01 |
| b4 | 1.513 | 1.00 | 0.51975383 | 2.91 | 1.30 |
| b1-1 | –0.178 | 1.25 | 0.77963074 | –0.23 | 82.3 |
| b2-2 | 0.276 | 1.25 | 0.77963074 | 0.35 | 73.0 |
| b3-3 | 4.985 | 1.25 | 0.77963074 | 6.39 | <0.01 |
| b4-4 | –0.124 | 1.25 | 0.77963074 | –0.16 | 87.6 |
| b1-2 | 0.520 | 1.00 | 0.90024003 | 0.58 | 57.4 |
| b1-3 | –2.185 | 1.00 | 0.90024003 | –2.43 | 3.19 |
| b2-3 | –3.420 | 1.00 | 0.90024003 | –3.80 | 0.253 |
| b1-4 | 0.323 | 1.00 | 0.90024003 | 0.36 | 72.6 |
| b2-4 | 0.505 | 1.00 | 0.90024003 | 0.56 | 58.5 |
| b3-4 | –2.123 | 1.00 | 0.90024003 | –2.36 | 3.62 |

Table 3
Box–Behnken design matrix with 4 independent factors (expressed codes) and response [$q_{total}$ (mg)] for fixed-bed column

| Run | Experimental values | | | | Coded values | | | | $Y_1$ |
|---|---|---|---|---|---|---|---|---|---|
| | Flow rate (mL/min) | Bed height (cm) | Particles size (μm) | $C_0$ (mg/L) | $X_1$ | $X_2$ | $X_3$ | $X_4$ | $q_{total}$ (mg) |
| 1 | 2 | 1 | 525 | 12.5 | –1 | –1 | 0 | 0 | 0.98 |
| 2 | 8 | 1 | 525 | 12.5 | 1 | –1 | 0 | 0 | 2.03 |
| 3 | 2 | 4 | 525 | 12.5 | –1 | 1 | 0 | 0 | 2.95 |
| 4 | 8 | 4 | 525 | 12.5 | 1 | 1 | 0 | 0 | 6.08 |
| 5 | 2 | 2.5 | 50 | 12.5 | –1 | 0 | –1 | 0 | 9.14 |
| 6 | 8 | 2.5 | 50 | 12.5 | 1 | 0 | –1 | 0 | 18.85 |
| 7 | 2 | 2.5 | 1,000 | 12.5 | –1 | 0 | 1 | 0 | 0.91 |
| 8 | 8 | 2.5 | 1,000 | 12.5 | 1 | 0 | 1 | 0 | 1.88 |
| 9 | 2 | 2.5 | 525 | 5 | –1 | 0 | 0 | –1 | 1.22 |
| 10 | 8 | 2.5 | 525 | 5 | 1 | 0 | 0 | –1 | 2.51 |
| 11 | 2 | 2.5 | 525 | 20 | –1 | 0 | 0 | 1 | 2.44 |
| 12 | 8 | 2.5 | 525 | 20 | 1 | 0 | 0 | 1 | 5.02 |
| 13 | 5 | 1 | 50 | 12.5 | 0 | –1 | –1 | 0 | 7.60 |
| 14 | 5 | 4 | 50 | 12.5 | 0 | 1 | –1 | 0 | 22.80 |
| 15 | 5 | 1 | 1,000 | 12.5 | 0 | –1 | 1 | 0 | 0.76 |
| 16 | 5 | 4 | 1,000 | 12.5 | 0 | 1 | 1 | 0 | 2.82 |
| 17 | 5 | 1 | 525 | 5 | 0 | –1 | 0 | –1 | 1.01 |
| 18 | 5 | 4 | 525 | 5 | 0 | 1 | 0 | –1 | 3.04 |
| 19 | 5 | 1 | 525 | 20 | 0 | –1 | 0 | 1 | 2.03 |
| 20 | 5 | 4 | 525 | 20 | 0 | 1 | 0 | 1 | 6.08 |
| 21 | 5 | 2.55 | 50 | 5 | 0 | 0 | –1 | –1 | 9.42 |
| 22 | 5 | 2.5 | 1,000 | 5 | 0 | 0 | 1 | –1 | 0.94 |
| 23 | 5 | 2.5 | 50 | 20 | 0 | 0 | –1 | 1 | 18.85 |
| 24 | 5 | 2.5 | 1,000 | 20 | 0 | 0 | 1 | 1 | 1.88 |
| 25 | 5 | 2.5 | 525 | 12.5 | 0 | 0 | 0 | 0 | 2.83 |
| 26 | 5 | 2.5 | 525 | 12.5 | 0 | 0 | 0 | 0 | 4.55 |
| 27 | 5 | 2.5 | 525 | 12.5 | 0 | 0 | 0 | 0 | 1.52 |

Table 4
Analysis of variance (ANOVA) for response surface quadratic model for the prediction of bifenthrin removal efficiency in fixed-bed column system

| Source | Sum of square (SS) | df | Mean squares (MSS) | *F*-value | *p*-value probability (*P*) > *F* |
|---|---|---|---|---|---|
| Model | 882.995 | 8 | 110.369 | 46.85 | 0.000 |
| Flow rate (mL/min) – $X_1$ | 29.234 | 1 | 29.234 | 12.41 | 0.002 |
| Bed height (cm) – $X_2$ | 69.216 | 1 | 69.216 | 29.38 | 0.000 |
| Particles size (μm) – $X_3$ | 507.130 | 1 | 507.130 | 215.28 | 0.000 |
| Feed concentration (mg/L) – $X_4$ | 27.482 | 1 | 27.482 | 11.67 | 0.003 |
| $X_1X_3$ | 19.097 | 1 | 19.097 | 8.11 | 0.011 |
| $X_2X_3$ | 46.786 | 1 | 46.786 | 19.86 | 0.000 |
| $X_3X_4$ | 18.020 | 1 | 18.020 | 7.65 | 0.013 |
| $X_3^2$ | 165.990 | 1 | 165.990 | 70.46 | 0.000 |
| Residual | 42.403 | 18 | 2.356 | | |
| Lack of fit | 37.784 | 16 | 2.362 | 1.02 | 0.603 |
| Pure error | 4.618 | 2 | 2.309 | | |
| Total | 925.357 | 26 | | | |
| $R^2$ | 0.958 | – | – | – | – |
| $R_{adj.}$ | 0.909 | – | – | – | – |

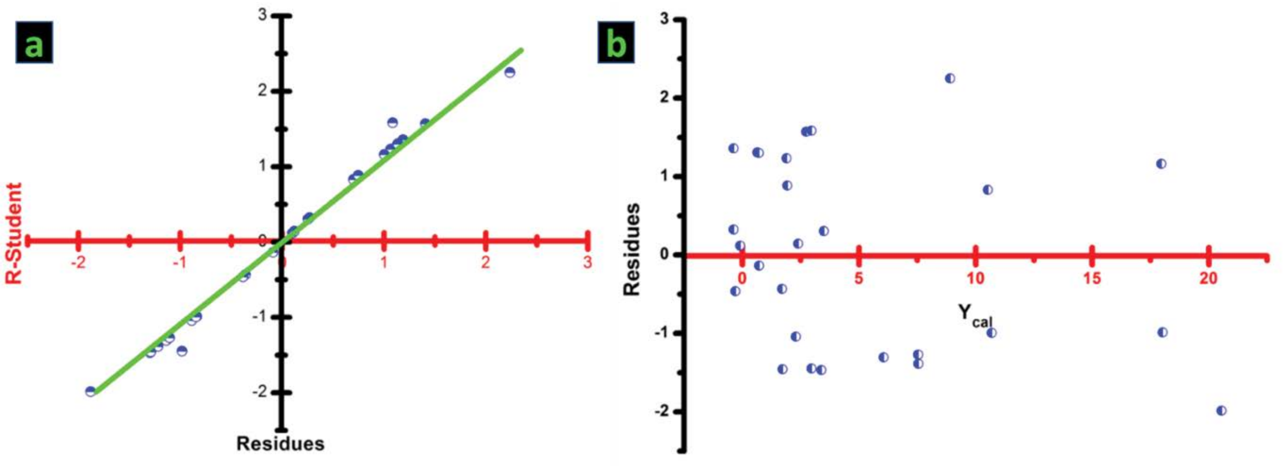


Fig. 8. (a) Plot of raw residuals vs. case number. (b) Normal probability of the residuals in fixed-bed column optimization.

by 1–4 cm. The specific surface area changes at a reason of 158 m² for each gram of TGTS. The increase in the specific surface area provides a higher number of active sites responsible for the binding of pesticide molecules which explains the increase in the amount of bifenthrin removed ($q_{total}$) as a function of bed height. Also, at higher bed heights, the mass transfer zone (MTZ) becomes wider and requires more time to reach the exit of the column which increases the breakthrough and exhaustion times and provides a higher residence time in the fixed-bed. The increase in the residence time of bifenthrin solution promotes a greater mass transfer mechanism and therefore makes the amount retained by the TGTS biomaterial higher. Identical results were deduced by Yusuf et al. [36] who worked on adsorption modeling of heavy metals ($Cu^{2+}$ and $Mn^{2+}$) onto modified graphene-based adsorbent. The authors in this study showed that the adsorbed amount increased from 30.03 to 48.83 mg/g and from 29.84 to 45.62 mg/g by increasing bed height from 1 to 3 cm for $Cu^{2+}$ and $Mn^{2+}$, respectively.

On the other hand, particles size is a parameter that significantly influences the mass of bifenthrin adsorbed on the TGTS biosorbent. With a larger particles size (1,000 μm), the residence time of the solute in the column decreases and the solution is, therefore, more likely to leave the column before equilibrium is reached. However, with smaller particles size (50 μm), the residence time of the solute in the column becomes longer, which favors mass transfer phenomena and allows the adsorption equilibrium to be established. The retention of bifenthrin molecules is therefore more favorable with a smaller particles size. The same conclusions were described by Sivarajasekar et al. who conducted several studies on the removal of dyes, fluorine and pesticides from aqueous solutions using batch and fixed-bed adsorption. Sivarajasekar et al. reported that increasing particles size

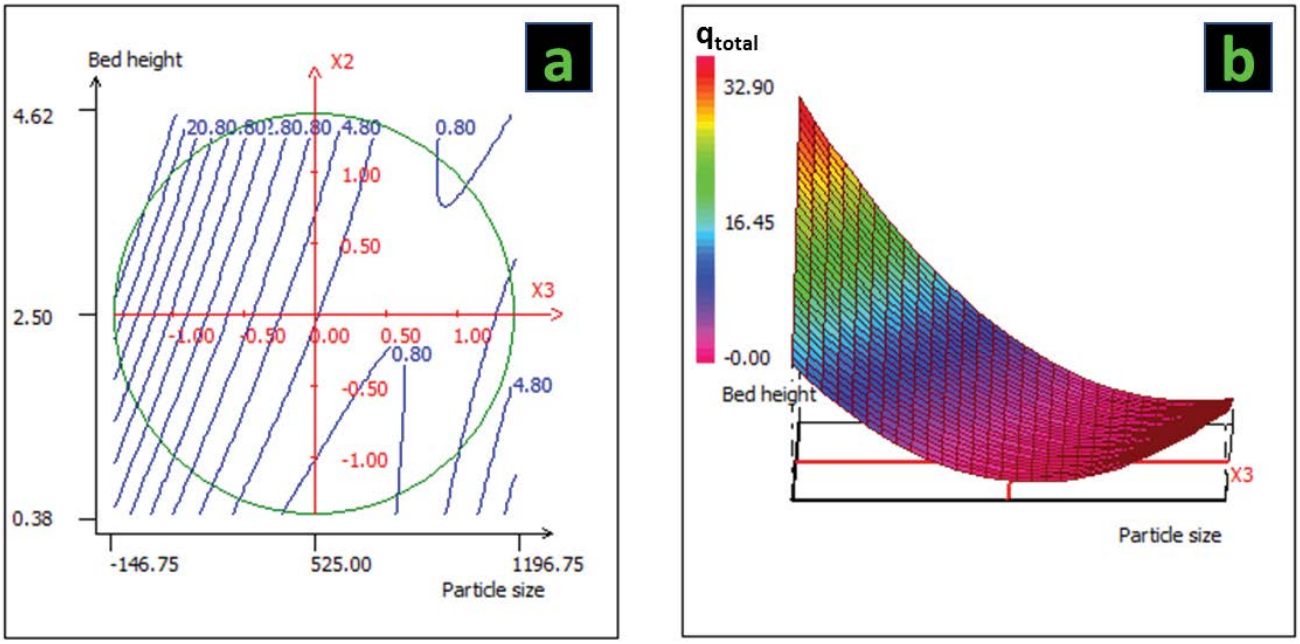


Fig. 9. Response surface 2D (a) and 3D (b) plots of the interactive effects of particles size and bed height.

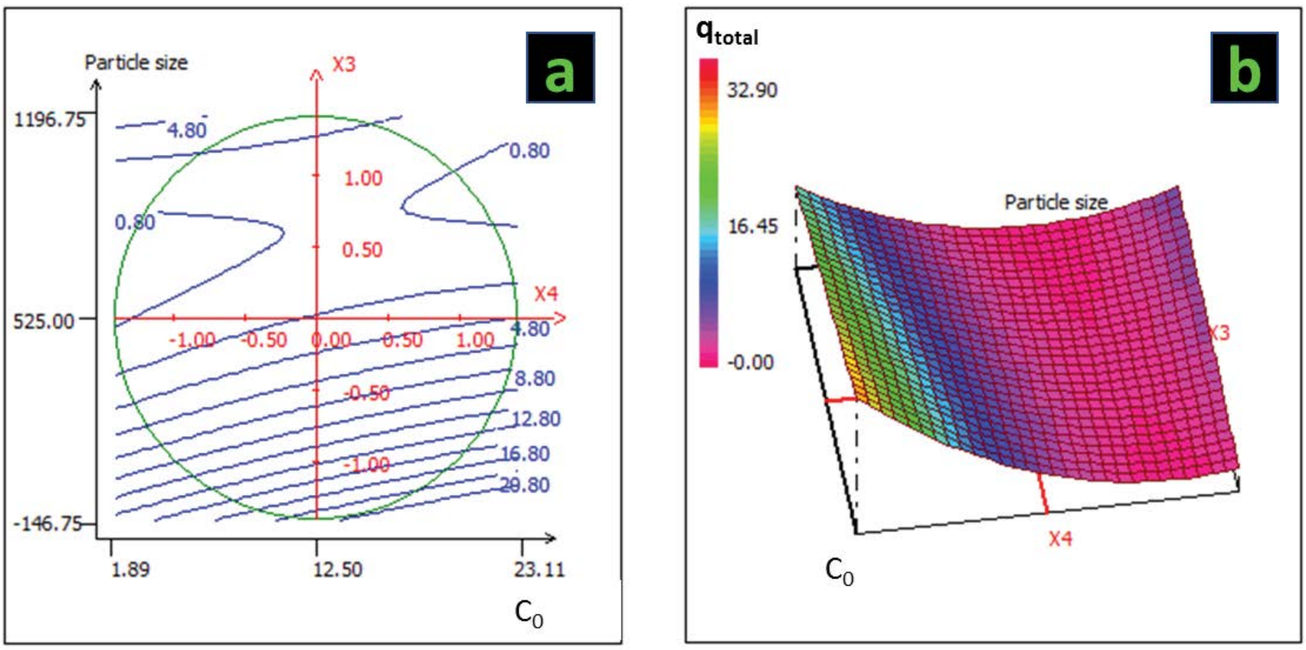


Fig. 10. Response surface 2D (a) and 3D (b) plots of the interactive effects of particles size and initial concentration.

decreases the available surface area and therefore decreases the amount retained as a pollutant [23,37,38]. Consequently, bed height and particles size directly affect the residence time and mass transfer of bifenthrin molecules in the bed column.

Fig. 10 reveals the interactive effect of bifenthrin feed concentration and particles size at a constant bed height ($L$ = 2.5 cm) and flow rate ($Q$ = 5 mL/min). As shown in this figure, ($q_{total}$) increases by increasing the feed concentration and decreasing the particles size. Typically, in a fixed-bed column, breakthrough and exhaustion times are reached earlier at high inlet concentrations because the binding sites become saturated. As inlet concentrations decrease, breakthrough and exhaustion times will be more important because transport is slow due to a decrease in the diffusion coefficient [39]. Thermodynamic factors determine the equilibrium distribution of the solute between the solid and liquid phases which explains why the amount adsorbed

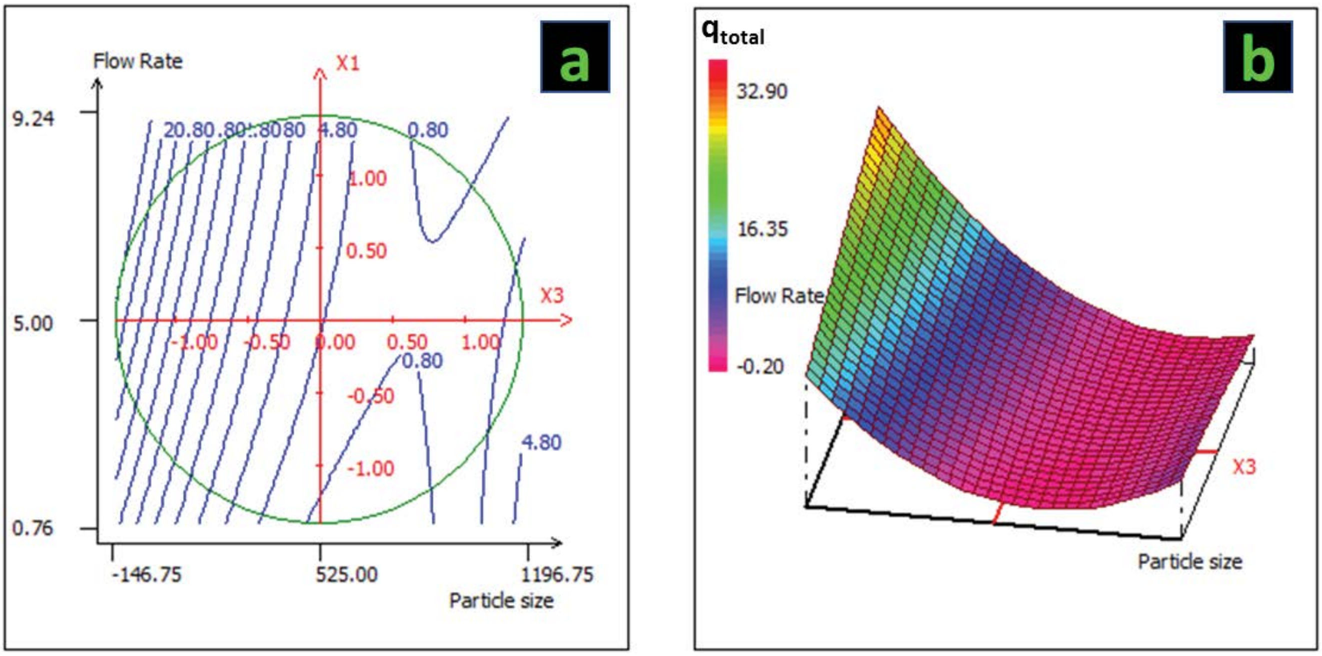


Fig. 11. Response surface 2D (a) and 3D (b) plots of the interactive effects of particles size and flow rate.

increases at high feeding concentrations [40]. Thus, in a fixed-bed column, under equilibrium conditions and at concentrations below saturation, the concentration of the solute in the solid phase is equal to its concentration in the feed solution. Therefore, the amount of bifenthrin adsorbed on the solid phase increases with increasing concentration of bifenthrin in the liquid phase. Identical conclusions were drawn by Yang et al. [41] who optimized the removal of linear olefins on microporous molecular sieves. The authors showed that the amount adsorbed increased from 176.9 to 251.0 mg/g, increasing the feed concentration by 20%–40%.

We have previously explained how the particles size influences the residence time of the solution to be treated in the column. It can therefore be deduced that the feed concentration and particles size affect the equilibrium conditions of the system.

Fig. 11 shows the interactive effect of flow rate ($Q$) and particles size (Ps) at a constant bed height ($L$ = 2.5 cm) and feed concentration ($C_0$ = 12.5 mg/L). Generally, if the increase in flow rate promotes the adsorption process, it can be suggested that diffusion into the external layer is the step that controls the adsorption process thereby increasing the speed reduces the layer thickness of the stagnant liquid film around the adsorbent particles. Otherwise, if the flow rate has no effect on adsorption, it can be assumed that the process is controlled by the internal diffusion step [42]. Fig. 11 shows that at a constant influent concentration (12.5 mg/L) and bed height (2.5 cm), the adsorbed amount of bifenthrin in the column increase with increasing flow rate [43]. Based on previous data, the adsorption of bifenthrin on TGTS biomaterial is governed by the external diffusion step. Increasing the flow rate also decreases the breakthrough and exhaustion times and increases the slope of the breakthrough curve. Increasing the slope and decreasing the breakthrough and exhaustion times reduces the resistance to mass transfer in the external layer and therefore the retention of the bifenthrin pesticide becomes more favorable. Based on the above findings, it can be understood that the interaction of flow rate and particles size significantly affects the adsorption of bifenthrin on TGTS biomaterial. The same results were reported by Marin et al. who removed glyphosate by graphene-$MnFe_2O_4$ using fixed-bed adsorption. The retained mass of glyphosate in this study increased from 3.90 to 5.49 mg/g with an increase in flow rate from 4 to 8 mL/min.

Modeling the removal of bifenthrin by TGTS biomaterial at optimal factor levels, including flow rate of 5 mL/min, bed height of 4 cm, particles size of 50 μm, and feed concentration of 12.5 mg/L, predicts that the amount removed will reach a value equal to $q_{total}$ = 22.80 mg.

## 4. Conclusion

The objective of this study is the modeling and optimization of dynamic fixed-bed column adsorption of bifenthrin pesticide on TGTS-based biomaterial. The characterization of the TGTS biomaterial reveals a calcium carbonate-based structure with a high specific surface area. This study shows that all independent factors, Ps, $L$, $Q$, $C_0$, significantly affect the removal efficiency of bifenthrin on TGTS. Strong interactions exist in the pairs (Ps-$L$), (Ps-$Q$), and (Ps-$C_0$). The order of significance of the effects is as follows: Ps > $L$ > (Ps-$L$) > $Q$ > $C_0$ > (Ps-$Q$) > (Ps-$C_0$). The highest predicted amount of bifenthrin removed by the TGTS biomaterial ($q_{total}$ = 22.80 mg) is obtained at the following optimal factor levels: flow rate of 5 mL/min, bed height of 4 cm, particle size of 50 μm, and feed concentration of 12.5 mg/L. RSM based on the Box–Behnken design is one of the most appropriate methods for establishing the best operating conditions for removing bifenthrin from aqueous solutions. The present study can be used as a guide for designing the removal of other pesticides under different experimental conditions using the TGTS biomaterial.

## References


[1] X. Zhang, Y. Luo, M. Zhang, K.S. Goh, Modeling the Effectiveness of Management Practices for Reducing Pesticide Residues in Surface Water, in Pesticides in Surface Water: Monitoring, Modeling, Risk Assessment, and Management, ACS Publications, 2019, pp. 233–258.

[2] H. Kaneko, Pyrethroids: mammalian metabolism and toxicity, J. Agric. Food Chem., 59 (2011) 2786–2791.

[3] W. Tang, D. Wang, J. Wang, Z. Wu, L. Li, M. Huang, S. Xu, D. Yan, Pyrethroid pesticide residues in the global environment: an overview, Chemosphere, 191 (2018) 990–1007.

[4] S.S. Albaseer, Factors controlling the fate of pyrethroids residues during post-harvest processing of raw agricultural crops: an overview, Food Chem., 295 (2019) 58–63.

[5] P. Bhatt, Y. Huang, H. Zhan, S. Chen, Insight into microbial applications for the biodegradation of pyrethroid insecticides, Front. Microbiol., 10 (2019) 01778, doi: 10.3389/fmicb.2019.01778.

[6] A.R. Ribeiro, O.C. Nunes, M.F.R. Pereira, A.M.T. Silva, An overview on the advanced oxidation processes applied for the treatment of water pollutants defined in the recently launched Directive 2013/39/EU, Environ. Int., 75 (2015) 33–51.

[7] L. Ghimici, I.A. Dinu, Removal of some commercial pesticides from aqueous dispersions using as flocculant a thymine-containing chitosan derivative, Sep. Purif. Technol., 209 (2019) 698–706.

[8] C. Fan, H. Dong, Y. Liang, J. Yang, G. Tang, W. Zhang, Y. Cao., Sustainable synthesis of HKUST-1 and its composite by biocompatible ionic liquid for enhancing visible-light photocatalytic performance, J. Cleaner Prod., 208 (2019) 353–362.

[9] Q. Wang, L. Chen, Y. Li, J. Yang, R. Yang, X. Yang, Magnetic nanocomposite-based TpPa-$NO_2$ covalent organic framework for the extraction of pyrethroid insecticides in water, vegetable, and fruit samples, Food Anal. Methods, 16 (2023) 71–82.

[10] M. Cobas, J. Meijide, M. Sanromán, M. Pazos, Chestnut shells to mitigate pesticide contamination, J. Taiwan Inst. Chem. Eng., 61 (2016) 166–173.

[11] M.J. Amiri, M. Bahrami, B. Beigzadeh, A. Gil, A response surface methodology for optimization of 2,4-dichlorophenoxyacetic acid removal from synthetic and drainage water: a comparative study, Environ. Sci. Pollut. Res., 25 (2018) 34277–34293.

[12] M.J. Amiri, M. Bahrami, F. Dehkhodaie, Optimization of Hg(II) adsorption on bio-apatite based materials using CCD-RSM design: characterization and mechanism studies, J. Water Health, 17 (2019) 556–567.

[13] A. Bakka, R. Mamouni, N. Saffaj, A. Laknifli, A. Benlhachemi, B. Bakiz, M. El Haddad, M. Ait Taleb, A. Roudani, A. Faouzi, The treated eggshells as a new biosorbent for elimination of carbaryl pesticide from aqueous solutions: kinetics, thermodynamics and isotherms, Sci. Study Res.: Chem. Chem. Eng. Biotechnol. Food Ind., 17 (2016) 271–278.

[14] A. Bakka, M. Ait Taleb, N. Saffaj, A. Laknifli, R. Mamouni, A. Benlhachemi, B. Bakiz, Y. Diane., Patellidae shells waste as a biosorbent for the removal of aldrin pesticide from aqueous solutions, J. Eng. Sci. Technol., 13 (2018) 925–942.

[15] M.A. Baih, H. Saffaj, K. Aziz, A. Bakka, N. El Baraka, H. Zidouh, R. Mamouni, N. Saffaj, Statistical optimization of the elaboration of ceramic membrane support using Plackett–Burman and response surface methodology, Mater. Today Proc., 52 (2022) 128–136.

[16] A. Hethnawi, M. Alnajjar, A.D. Manasrah, A. Hassan, G. Vitale, R. Jeong, N.N. Nassar, Metformin removal from water using fixed-bed column of silica-alumina composite, Colloids Surf., A, 597 (2020) 124814, doi: 10.1016/j.colsurfa.2020.124814.

[17] T.M.S. Attia, X.L. Hu, Synthesized magnetic nanoparticles coated zeolite for the adsorption of pharmaceutical compounds from aqueous solution using batch and column studies, Chemosphere, 93 (2013) 2076–2085.

[18] M.A. Baih, N. Saffaj, A. Bakka, R. Mamouni, H. Zidouh, N. El Qacimi, Clay ceramic support membrane optimization using factorial design approach, J. Appl. Membr. Sci. Technol., 25 (2021) 1–15.

[19] N. Sivarajasekar, N. Mohanraj, R. Baskar, S. Sivamani, Fixed-bed adsorption of ranitidine hydrochloride onto microwave assisted—activated *Aegle marmelos correa* fruit shell: statistical optimization and breakthrough modelling, Arabian J. Sci. Eng., 43 (2018) 2205–2215.

[20] M.A. Baih, N. El Qacemi, H. Zidouh, A. Bakka, N. El Baraka, R. Mamouni, N. Saffaj, Elaboration of $TiO_2$ ultrafiltration membrane deposited on Moroccan Sahara Clay, E3S Web Conf., 229 (2021) 01033, doi: 10.1051/e3sconf/202122901033.

[21] H.E. Reynel-Avila, D.I. Mendoza-Castillo, A. Bonilla-Petriciolet, J. Silvestre-Albero, Assessment of naproxen adsorption on bone char in aqueous solutions using batch and fixed-bed processes, J. Mol. Liq., 209 (2015) 187–195.

[22] M.A. Baih, H. Saffaj, A. Adam, A. Bakka, N. El Baraka, H. Zidouh, R. Mamouni, N. Saffaj, Application of the experimental design for the optimization of microfiltration membrane, J. Appl. Membr. Sci. Technol., 26 (2022) 95–106.

[23] N. Sivarajasekar, K. Balasubramani, N. Mohanraj, J.P. Maran, S. Sivamani, P.A. Koya, V. Karthik, Fixed-bed adsorption of atrazine onto microwave irradiated *Aegle marmelos correa* fruit shell: statistical optimization, process design and breakthrough modeling, J. Mol. Liq., 241 (2017) 823–830.

[24] M.A. Baih, H. Saffaj, A. Adam, A. Bakka, H. Zidouh, R. Mamouni, N. Saffaj, Processing and characterization of titania ultrafiltration ceramic membrane: response surface methodology optimization, Desal. Water Treat., 257 (2022) 96–109.

[25] A. Bakka, R. Mamouni, N. Saffaj, A. Laknifli, K. Aziz, A. Roudani, Removal of bifenthrin pesticide from aqueous solutions by treated patellidae shells using a new fixed-bed column filtration technique, Process. Saf. Environ. Prot., 143 (2020) 55–65.

[26] J.A. Onimisi, R. Ismail, K.S. Ariffin, N. Baharun, H.B. Hussin, A novel rapid mist spray technique for synthesis of single phase precipitated calcium carbonate using solid-liquid-gas process, Korean J. Chem. Eng., 33 (2016) 2756–2760.

[27] J. Chen, M. Hamon, H. Hu, Y. Chen, A. Rao, P. Eklund, R. Haddon, Solution properties of single-walled carbon nanotubes, Science, 282 (1998) 95–98.

[28] M. Ehrampoush, G. Ghanizadeh, M. Ghaneian, Equilibrium and kinetics study of Reactive red 123 dye removal from aqueous solution by adsorption on eggshell, J. Environ. Health Sci. Eng., 8 (2011) 101–106.

[29] M. Elkady, A.M. Ibrahim, M. Abd El-Latif, Assessment of the adsorption kinetics, equilibrium and thermodynamic for the potential removal of Reactive red dye using eggshell biocomposite beads, Desalination, 278 (2011) 412–423.

[30] Z. Zhao, L. Zhang, H. Dai, Y. Du, X. Meng, R. Zhang, Y. Liu, J. Deng, Surfactant-assisted solvo-or hydrothermal fabrication and characterization of high-surface-area porous calcium carbonate with multiple morphologies, Microporous Mesoporous Mater., 138 (2011) 191–199.

[31] M. Abdel-Khalek, M.A. Rahman, A. Francis, Exploring the adsorption behavior of cationic and anionic dyes on industrial waste shells of egg, J. Environ. Chem. Eng., 5 (2017) 319–327.

[32] W.-F. Ho, H.-C. Hsu, S.-K. Hsu, C.-W. Hung, S.-C. Wu, Calcium phosphate bioceramics synthesized from eggshell powders through a solid state reaction, Ceram. Int., 39 (2013) 6467–6473.

[33] Z. Wei, C. Xu, B. Li, Application of waste eggshell as low-cost solid catalyst for biodiesel production, Bioresour. Technol., 100 (2009) 2883–2885.

[34] J.S. Noh, J.A. Schwarz, Estimation of the point of zero charge of simple oxides by mass titration, J. Colloid Interface Sci., 130 (1989) 157–164.

[35] M. Shirzad-Siboni, A. Khataee, F. Vafaei, S.W. Joo, Comparative removal of two textile dyes from aqueous solution by adsorption onto marine-source waste shell: kinetic and isotherm studies, Korean J. Chem. Eng., 31 (2014) 1451–1459.

[36] M. Yusuf, K. Song, L. Li, Fixed-bed column and artificial neural network model to predict heavy metals adsorption dynamic on surfactant decorated graphene, Colloids Surf., A, 585 (2020) 124076, doi: 10.1016/j.colsurfa.2019.124076.
[37] N. Sivarajasekar, T. Paramasivan, S. Muthusaravanan, P. Muthukumaran, S. Sivamani, Defluoridation of water using adsorbents-a concise review, J. Environ. Biotechnol. Res., 6 (2017) 186–198.
[38] N. Sivarajasekar, R. Baskar, T. Ragu, K. Sarika, N. Preethi, T. Radhika, Biosorption studies on waste cotton seed for cationic dyes sequestration: equilibrium and thermodynamics, Appl. Water Sci., 7 (2017) 1987–1995.
[39] B. Hayati, A. Maleki, F. Najafi, F. Gharibi, G. McKay, V.K. Gupta, S.H. Puttaiah, N. Marzban, Heavy metal adsorption using PAMAM/CNT nanocomposite from aqueous solution in batch and continuous fixed-bed systems, Chem. Eng. J., 346 (2018) 258–270.
[40] D.M. Ruthven, Principles of Adsorption and Adsorption Processes, John Wiley & Sons, New York, 1984.
[41] R. Yang, R. Gao, Z. Qian, Y. Wang, Batch and fixed-bed column selective adsorption of $C_6$, $C_8$ and $C_{10}$ linear α-olefins from binary liquid olefin/paraffin mixtures onto 5A and 13X microporous molecular sieves, Sep. Purif. Technol., 230 (2020) 115884, doi: 10.1016/j.seppur.2019.115884.
[42] H.S. Fogler, M. Gürmen, Elements of Chemical Reaction Engineering, 3rd ed., Prentice Hall, New Jersey, 1999.
[43] D.-M. Guo, Q.-D. An, R. Li, Z.-Y. Xiao, S.-R. Zhai, Ultrahigh selective and efficient removal of anionic dyes by recyclable polyethylenimine-modified cellulose aerogels in batch and fixed-bed systems, Colloids Surf., A, 555 (2018) 150–160.